

1
2
3
4
5
6
7
8
9
10

Original Research Article
**Mass Balance of the Himalayan Glaciers and their
Regional Variations**

ABSTRACT

Aim: Popular methods of glacial mass balance studies are time consuming, laborious and therefore, not repetitive at yearly manner. A compact, user-friendly classification algorithm has been applied to estimate Equilibrium Line Altitude (ELA) and Mass balance of mountain or valley glaciers at yearly basis using Synthetic Aperture Radar (SAR) data. Cloud cover over the glacier catchment areas was studied to identify major seasons of precipitation over the study areas. The results were also compared to study the regional characteristics of the glaciers.

Study Area: The proposed module was used to analyze data over three Himalayan glaciers, namely, Durung Drung, Gangorti and Zemu. Chhota Shigri glacier was also studied with these three glaciers to understand the regional variations of the Himalayan glaciers.

Methodology: The classification algorithm was fixed for all glaciers and also independent from season, therefore, required least user intervention. The conditional loop based logics, consist of linear equations, classified glaciated region in different physical zones. Purely backscatter based classification result produced error by mixing zones due to overlapped signatures. Altitude thresholds of accumulation zones were employed to segregate the mixing in next level. The method required calibrated ortho-rectified sigma naught dual-pol SAR imagery as primary input. The glaciated area should be provided as Area of Interest (AOI). A Digital Elevation Model (DEM) file is required for altitude threshold. The output classes are saved in separate files with Boolean values. Optical data were used to estimate cloud coverage over the catchments of the glaciers.

Result: Average mass balance of the selected glaciers is estimated as $-0.44 \text{ m w.e.a}^{-1}$ during the study period. The mass balance of the glaciers are comparatively studied with variation in melting seasons, duration of melting periods, on set and cease of melting for each glacier to understand the regional pattern of mass loss.

Conclusion: Co and cross polarized SAR data are employed to derived debris size; however, cross polarized SAR backscattering has better correlation with debris size. The accuracy of the result derived from the developed method is $\pm 50 \text{ mm}$. Collection of field data on the surface topography is difficult for Mountain glaciers, especially over Himalaya. Use of satellite data can generate detailed information of glacier surface which will be further help to understand role of debris in glacier mass balance.

11 *Keywords: Synthetic Aperture Radar (SAR), snow line, Firm line, ELA, mass balance,*
12 *cloud cover.*

13 **1. INTRODUCTION**

14
15 The Himalayan glaciated region accompanying the other neighboring glaciated regions, like,
16 Karakoram, Hindukush and Central Asian mountain range, forms the largest glaciated region
17 outside the poles. The major agricultural regions of Asia depend on the perennial rivers
18 originated from the snow-melt runoff of this glaciated region. Therefore, the health of the
19 Himalayan and other neighboring glaciated regions are of a major concern for the glaciologists
20 to understand the impact of the climate change over these regions. In last few decades,
21 advancement of the remote sensing techniques, promote glaciological studies which are,
22 otherwise, a tedious job because of the harsh environment and climatic conditions. Various

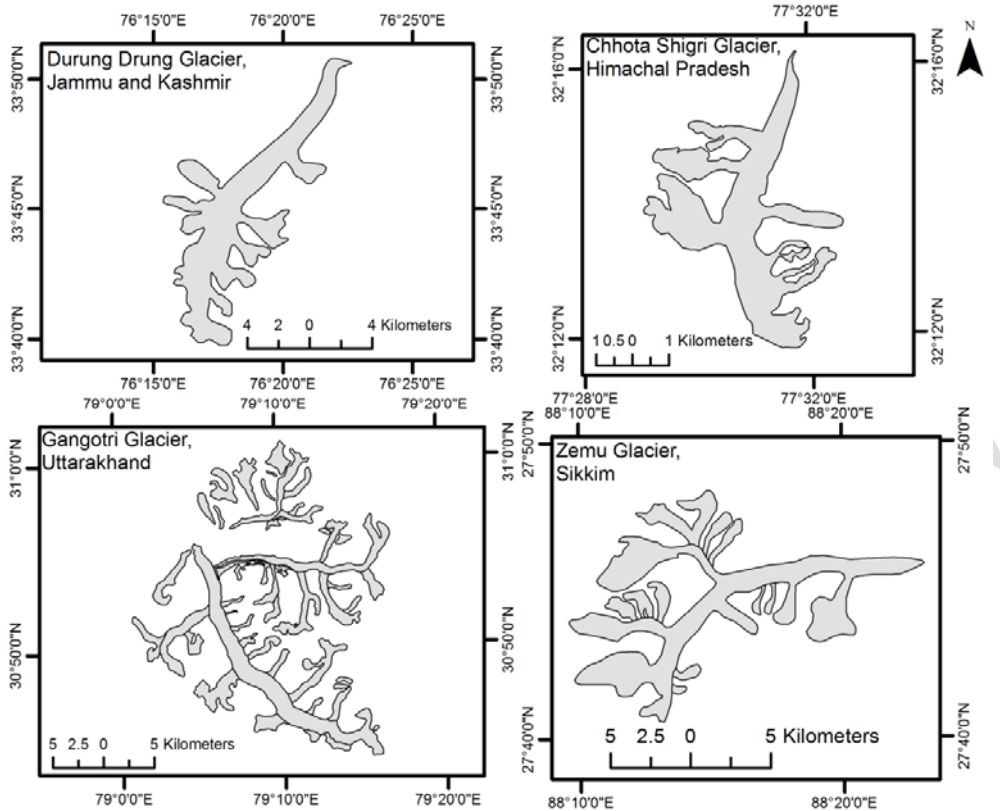
23 research works published on estimation of mass balances of the Himalayan glaciers explain the
24 glaciers are losing mass, however, their rate of losses are debatable. The mass balance rates of
25 the Chhota Shigri glacier of the Himachal Himalaya differently reported by a variety of study
26 methods [1 – 6]. This variability is more prominent for the glaciers of one glaciated basin to
27 others [7 – 9]. The fact of loosing mass of the Himalayan glaciers is quite established, however,
28 in contrast, the glaciers of the Karakoram region are advancing due to a positive mass balance.
29 Statistically significant increase in winter and summer precipitation have been observed since
30 1961, which indicate winter warming and summer cooling and increase in the summer
31 cloudiness and storms. This contributes to the positive mass balance [10, 11]. Most of the mass
32 balance studies are objected to study one or two glaciers at a time and the methods involved in
33 estimation are also repetitive for each different glacier and hence, time-consuming which may
34 restrict selection of study areas.

35 Here, this research work has been objected to estimate mass balance of the Himalayan glaciers
36 using a single geo-informatics tool which reduces processing time and also subjectivity of the
37 users. The output classified SAR images provide information like snowline, firnline, on set and
38 cease of melting season. The second level products generated from this information are
39 Equilibrium Line Altitude (ELA) and mass balance. The Himalayan glaciers found at different
40 basins from west to east are studied using C band Synthetic Aperture Radar (SAR) data during
41 2012 to 2015. Use of C band (5.35 GHz) SAR makes the study independent of the atmospheric
42 conditions (cloud cover) and solar illumination (day and night), unlike, optical data. Application
43 of a tool to estimate mass balances of different glaciers will also allow a comparative study of
44 the mass balance values of the selected glaciers.

45 46 **2. STUDY AREA**

47
48 The Study areas are selected considering factors, like, differences in latitudes and longitudes,
49 location of the glaciers on the ridgeline and amount of rainfall (summer and winter). Three
50 Himalayan glaciers are selected from west to east (Figure 1). The geographical positions of the
51 glaciers show the longitudinal difference of the glaciers is more than 10 degrees and 6 degrees
52 in latitude. The differences in precipitation amounts are also prominent over these regions [12].
53 The ridgelines of the Himalaya, oriented in east - west direction, controls amount of rainfall by
54 creating orographic effect over the south-east monsoonal wind. During summer monsoon, the
55 southern sides of the ridges get more precipitation than lee side. It is opposite for winter
56 precipitation. Based on these differences the study areas are selected. The glaciers are
57 distributed from west to east in different micro-climatic regions.

58 From the extreme western part of the Himalaya, the Durung Drung (DD) glacier of Jammu and
59 Kashmir State is selected. In the Garhwal Himalaya, the Gangotri (GG) glacier is selected as
60 another study area and is located at south-eastern side of the DD glacier. Both the monsoonal
61 and mid-latitude westerly precipitations influence the amount of precipitation [12]. In the eastern
62 Himalaya, the Zemu (ZM) glacier, which is originated from eastern flank of Kanchenjanga
63 peak, is studied as the fourth study area. The ZM glaciated area is dominated by monsoonal
64 precipitation. In the eastern region, around 80% of the mass is added by monsoonal
65 precipitation [13]. Chhota Shigri (CS) glacier of Himachal Pradesh is also studied for regional
66 variability study. Mass balance study of the Chhota Shigri glacier is already done by Das and
67 Chakraborty [6] using the same linear decision rule which is incorporated in the classification
68 tool stated in this paper.
69



70

71 **Fig. 1: Location map of the study areas; namely, a) Durung Drung (DD), b) Chhota Shigri**
 72 **(CS), c) Gangotri (GG) and d) Zemu (ZM).**

73

74

75

76

77

78

79

80

81

82

83

84

85

3. DATA AND METHODOLOGY

The Data of Synthetic Aperture Radar (SAR) sensor acquired in 5.35 GHz frequency (C band) were used as the primary input for monitoring the mass balances of the glaciers. A set of eighty nine dual polarimetric SAR scenes (HH and HV) of Medium Resolution SAR mode (MRS; 24 m resolution) of Radar Imaging SATellite-1 (RISAT-1) were collected over a period of 2012 - 2015 covering both ablation and accumulation seasons. The data, having nominal incidence angle of 37°, were geometrically corrected against the Digital Elevation Models to minimize the geometric errors (layover and foreshortening) generated due to the side looking properties of SAR over the glaciated regions. A description of the data used for the study is given in Table 1.

Table 1 Description of the data used for identifying glacial facies to derive mass balance.

Data Type	Satellite/Sensor	Remarks
C band SAR dual-pol (HH, HV)	RISAT-1 MRS mode	Resolution: spatial 25 m, temporal 25 days, nominal incidence: 37°
Optical data	Resourcesat-2 AWiFS, Landsat 7/8	AWiFS spatial resolution: 56 m x 56 m; Spectral band used: SWIR, NIR and Red.
Digital Elevation Model	SRTM DEM	Spatial resolution 30 m x 30 m
Glacier boundary as .shp format (vector file)	SRTM DEM	Developed from DEM and derivatives of DEM, i.e., slope and profile curvature (Chakraborty, Panigrahy and Kundu 2014)

86

87

The Speckle filtering and backscattering sigma naught calibration were the major pre-processing steps before classifying the images. Equation (1) was used for calibrating filtered

88 scenes to backscattering sigma naught values. A linear rule based classification algorithm
 89 developed by Kundu and Chakraborty [14] had been applied to classify the glacial zones of the
 90 glaciers. The inputs to the classification step were SAR data (filtered, calibrated ortho-rectified),
 91 glacier boundary (vector file, .shp format) to generate mask and DEM for providing altitude
 92 thresholds to separate out the classes having overlapped backscattering signatures. The output
 93 results contained different backscattering classes based on the surface roughness, moisture
 94 content and subsurface properties (during winter season only).

$$\sigma_o(\text{in dB}) = 20 \log_{10}(X) - \kappa_{dB} + 10 \log_{10}(\sin\theta_{\text{local}}/\sin\theta_{\text{centre}}), \quad \text{Equation (1)}$$

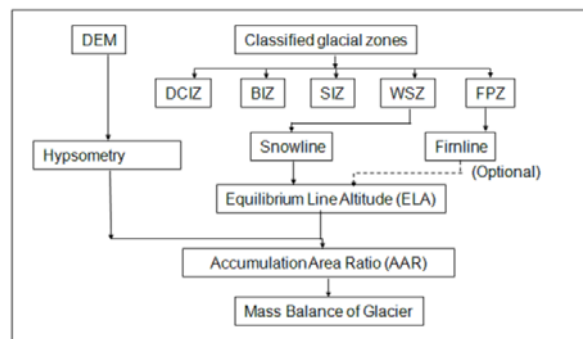
96 Where, X = amplitude value, κ_{dB} = Calibration constant, θ_{local} = local incidence angle at a pixel,
 97 θ_{centre} = nominal incidence angle at the scene centre.

100 The glacial facies, identified from the SAR data, were Debris Covered Ice Zone (DCIZ), Bare Ice
 101 Zone (BIZ) in the ablation zone and Superimposed Ice Zone (SIZ), Wet Snow Zone (WSZ),
 102 Partially Wet Snow Zone (WSZ2) and Seasonal Frozen Percolation Zone (Seasonal FPZ) in the
 103 accumulation zone. The snowline was considered as the lower altitude extent of the WSZ.
 104 Temporal changes of the snowline altitudes throughout the four years were derived from the
 105 classification results. The moisture content within the snow pack absorbs part of the incident
 106 radar energy and a large portion of it scatters in forward direction by specular reflection due to
 107 the concentration of water molecules at top surface of the snow pack. The WSZ, therefore,
 108 appears as the darkest zone over the glacier. The classification output during the ablation
 109 season provides distribution of the WSZs over the glaciers. The lower extents of the zone were
 110 identified and overlaid with DEM to extract the mean snowline altitudes. The highest snowline
 111 altitude at the end of ablation period (middle of August to middle of September months) is
 112 considered as the Equilibrium Line Altitude (ELA) of a particular glacier for a particular year. If
 113 data during this time period is not available, then the firn line altitude at the starting of the
 114 accumulation season of the same year is considered as the ELA for the glacier [6].

115 The compacted snow at the end of ablation season develops firn (density 0.5 kg m^{-3}). The
 116 granular snow acts as strong scatterers of the radar beam. This produces high backscattering
 117 and the firn zone appears bright in the SAR images. The zone is identified as the “Seasonal
 118 Frozen Percolation Zone” having a signature similarity with the ‘Frozen Percolation Zone’ during
 119 the winter season [14](Kundu and Chakraborty, 2015). The lower extent of the seasonal FPZ
 120 has been marked from the classified outputs and mean altitudes of the firn lines were derived
 121 similarly as done for the snow line altitudes.

122 The mass balance values (mb) were calculated from the ELAs by using an empirical method
 123 [15]. Before estimation, Accumulation Area Ratio (AAR), against each ELA for each glacier, was
 124 derived and used as an input in the empirical equation (2) (Figure 2).

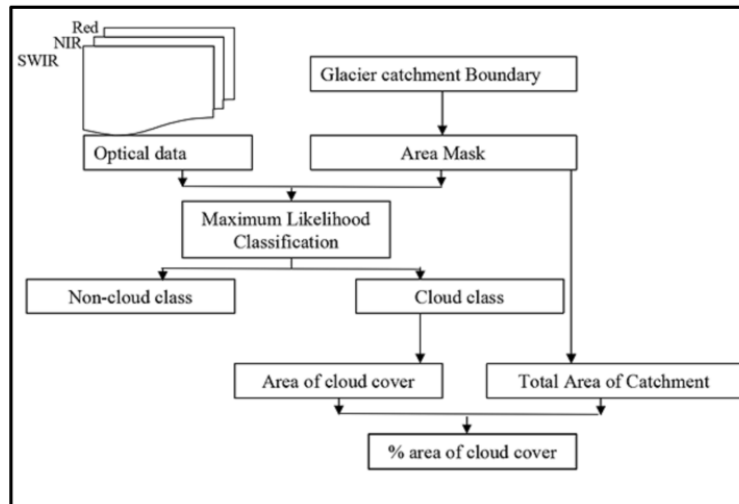
$$\text{Mb (m w.e.)} = (243.01 \times \text{AAR} - 120.187)/100 \quad \text{Equation (2)}$$



130 **Fig. 2: Methodology followed to derive snowline, firnline, Equilibrium Line Altitude (ELA),**
 131 **Accumulation Area Ratio (AAR) and mass balance.**

132 The optical satellite images of Resourcesat-2 AWiFS (Advanced Wide Field Sensor) and
 133 Landsat 7/8 were collected to snowline altitudes of the glaciers during the four-year study
 134 period. The data were also used to find out the percentage area of the glacier basins under
 135
 136

137 cloud cover for the year 2014 (Figure 3). The percentage area under cloud cover provides
 138 information on precipitation pattern and concentration over the glaciated basins from east to
 139 west. Short wave Infra-red bands of the optical data (SWIR) were used in the classification to
 140 reduce the error which was occurred in other optical bands by mixing of the signatures from
 141 snow and cloud. Error of the classification results increases in the presence of the ice clouds.
 142 However, the pattern of the cloud cover helps to reduce the mixing.

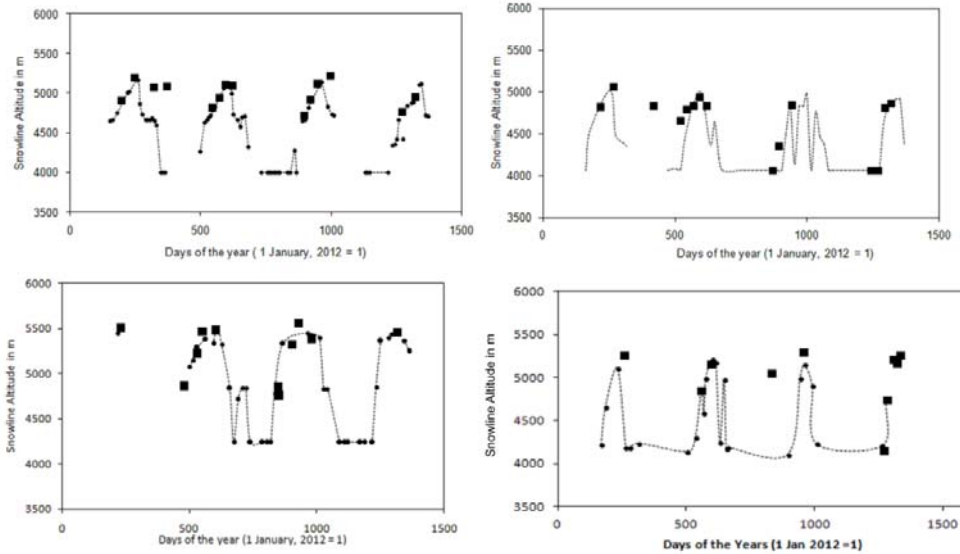


143 **Fig. 3: Methodology of cloud cover classification and derivation of percentage cloud**
 144 **cover area over glacier catchment.**

145
 146
 147 **4. RESULTS AND DISCUSSION**

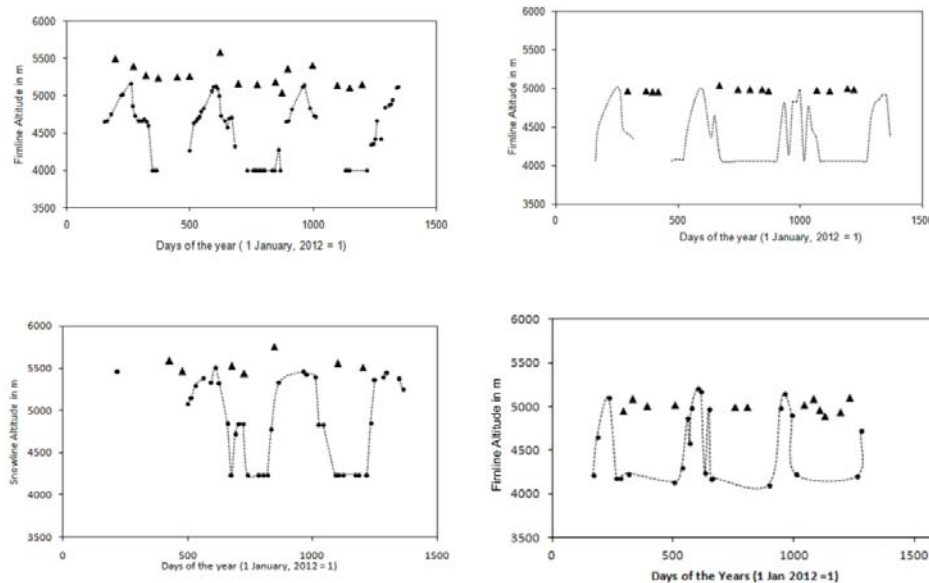
148
 149 **4.1 Temporal monitoring of Snowline and firn line altitudes**

150 The snow lines of the three Himalayan glaciers were identified from the classified SAR data of
 151 the ablation seasons. The optical data were also used independently to derive the snowlines.
 152 Figure 4 shows the temporal variability of the snowline altitudes of the three glaciers. As radar
 153 signals are sensitive to the presence of liquid water, changes within the snow cover due to
 154 melting identified. Over the DD glacier, melting starts from the month of June, whereas, the
 155 same has been observed during the month of April for the ZM glacier of the eastern Himalaya.
 156 The average onset of the melting period is experienced during the month of May.
 157



158
 159 **Fig. 4: Snowline altitudes derived from SAR data are represented by black squares.**
 160 **Dotted line with black circle is showing temporal changes in snowline altitudes identified**
 161 **by optical data. The graph includes snowline altitudes for four consecutive years from**
 162 **2012 to 2015.**

163
 164 Figure 5 shows the altitudes of the firn lines. Variability of altitude is not significant for the firn
 165 lines throughout the accumulation seasons. Yearly variation in the mean firn line altitude is also
 166 negligible. The altitudes of the firn lines during the onset of the accumulation season are closest
 167 to the altitudes of snow lines at the end of the ablation season of any particular year. The lowest
 168 limit of the firn zone defines the extent of the accumulation zone of a glacier. However, SAR
 169 also detects old firn layers and mixes with the newer one and appears almost at the similar
 170 altitude each year. Therefore, identification of the ELA from the firn line altitude during peak
 171 winter season can introduce error in the result. In long term study, extent of the firn zone,
 172 however, reveals advancement or retreat of the glacier. The average firn line altitude of the ZM
 173 glacier is around 5400 m whereas; the other three glaciers have firn lines at 4900 - 5000 m
 174 altitude range.
 175
 176



178 **Fig. 5: The Firn line altitudes of the four glaciers for four consecutive years from 2012 to**
 179 **2015 are shown in black triangles. The black dotted lines with black circles represent**
 180 **snowline altitudes of the four glaciers derived from optical data.**

181
 182 **4.2 Estimation of mass balance from ELA derived from SAR data**
 183 The ELAs of the three glaciers are derived from the highest snowline altitudes identified from
 184 the SAR derived classification outputs. Table 2 gives the ELAs of the three glaciers for the
 185 period of 2012 - 2015. The mass balance values are calculated from the ELAs by using the
 186 empirical method [15]. Table 3 is giving the mass balance values of the all these glaciers during
 187 2012 - 2015. Mass balance of the Chhota Shigri (CS) glacier for the same period of time has
 188 been added in the table to get a complete database to understand regional variations.

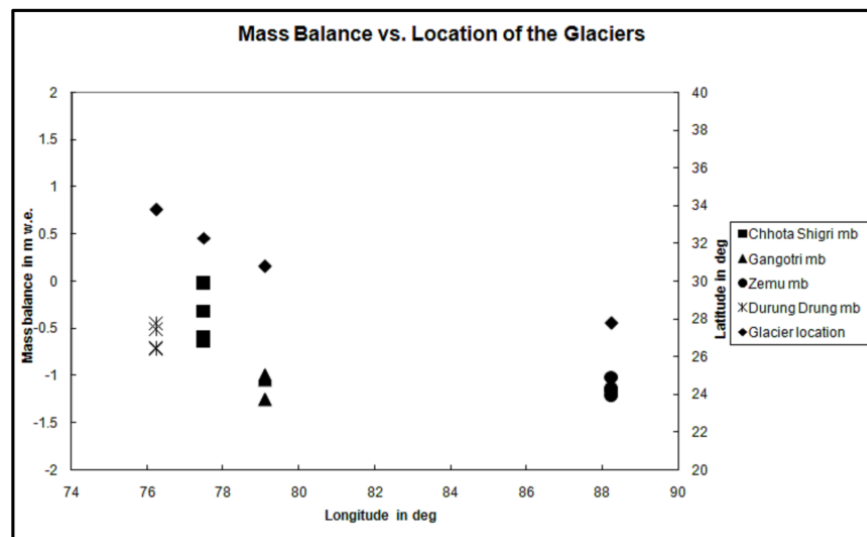
189
 190 **Table 2 ELA (in m) of the glaciers derived from the highest snowline altitudes estimated**
 191 **from the temporal analysis of SAR data for the period of 2012 to 2015. Highlighted**
 192 **altitudes are derived from firn line during onset if accumulation season.**

Year	Durung Drung (DD)	Chhota Shigri (CS) (Das and Chakraborty, 2019)	Gangotri (GG)	Zemu (ZM)
2012	5257	5028	5194	5517
2013	5151	5019	5103	5479
2014	5173	4973	5114	5385
2015	5251	4913	5118	5465

193
 194 **Table 3 Mass balances (in m w.e. a⁻¹) of four glaciers are derived from the ELA estimated**
 195 **from the SAR data.**

Year	Durung Drung (DD)	Chhota Shigri (CS) (Das and Chakraborty, 2019)	Gangotri (GG)	Zemu (ZM)
2012	-0.31	-0.65	-0.69	-0.66
2013	-0.12	-0.59	-0.51	-0.63
2014	-0.16	-0.25	-0.53	-0.52
2015	-0.3	-0.03	-0.54	-0.61

196
 197 In comparison to the central and eastern Himalayan glaciers, i.e., the GG and ZM, the western
 198 Himalayan glacier, the DD glacier, has better mass balance (Figure 6). The similar result has
 199 been represented by Bahuguna et al. [16].



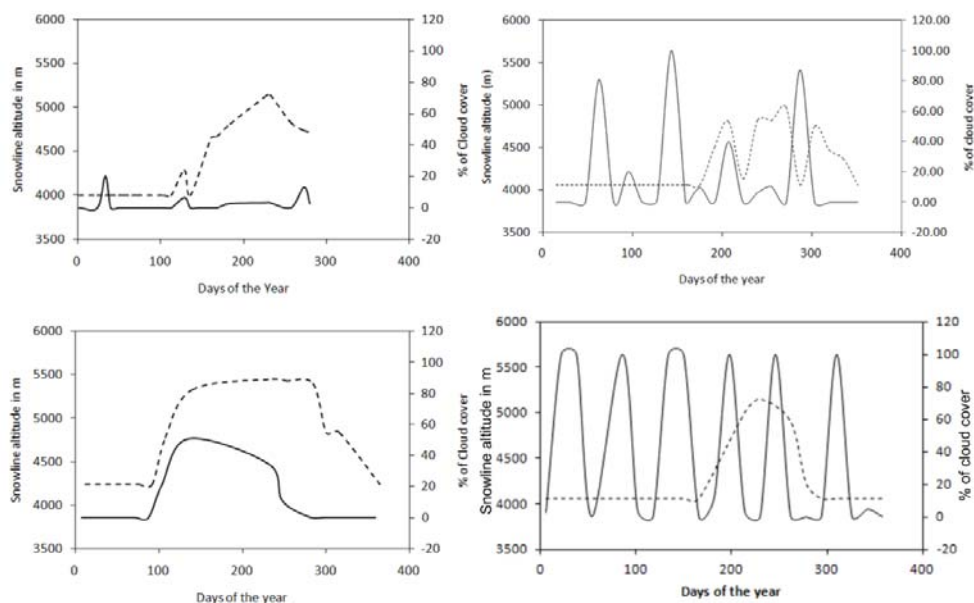
200
 201 **Fig. 6: Variation on mass balance figures (mb in m w.e.) compared with changes in**
 202 **geographical distributions. The star marks are showing geographical location (Lat/long)**
 203 **of the glaciers. Mass balance figures of four glaciers are when plotted against**
 204 **longitudinal positions the figures show that eastern and central Himalayan glaciers, i.e.,**

205 **Zemu and Gangotri have higher rate of losing mass as compared to western Himalayan**
206 **glaciers.**

208 **4.3 Effect of weather parameters over the region wise differences in mass**
209 **balance**

210 The relationship between mass balance and regional variation in climate are not yet established
211 firmly because of the insufficiency in weather and other ancillary data over the high altitude
212 Himalayan regions. The GG and ZM glaciers are situated at southern side of 30° N latitude and
213 the DD and CS glaciers are situated at north of it. Therefore, according to the latitudinal
214 differences, glaciers are distributed in two major climatic regions, i.e., tropical hot & humid and
215 mid-latitude alpine climatic zones. Throughout the longitudinal extension of the Himalaya,
216 precipitation varies from east to west according to the orographic monsoonal precipitation. The
217 meteorological weather stations are located at much lower altitudes compared with the terminal
218 altitudes of the glaciers. Automated weather stations are installed near some of the selected
219 glaciers in recent times; however, data on the variation in the weather parameters through the
220 complete stretch of the Himalaya are not available. Therefore, analysis on the cloud cover
221 concentration has been studied over the catchment areas of these selected glaciers. The
222 probability of precipitation (solid/liquid form) is high at the presence of the cloud cover. It has
223 been assumed that if the rate of cloud cover was high within a span of one year, the area would
224 have received higher amount of precipitation over the catchment area.

225 Figure 7 shows the percentage of the cloud cover area over the four glacier catchments for the
226 year 2014. The occurrence of complete cloud cover over the catchment area (100%) is highest
227 in the DD glacier for this selected year which decreased gradually over the other three glaciers
228 from west to east. The number of days under the cloud cover is also high for the DD glacier. A
229 higher occurrence of the cloud cover over the glacier catchment implies a higher probability of
230 precipitation throughout the year. Precipitation at the high altitude mostly occurs in solid form
231 which adds mass to the glacier. Situated in the rain shadow side of the Himalayan range and
232 opposite aspect with the monsoonal air flow the GG glacier catchment has least percentage of
233 cloud cover. The ZM glacier has maximum numbers of days of cloud cover which has around
234 50% coverage of the catchment area. Occurrence of the cloud cover is highly concentrated over
235 the ZM glacier during the ablation season. During the winter season, the glacier has minimum
236 cloud cover which implies minimum mass accumulation to the glacier during the accumulation
237 season. Therefore, for the ZM glacier, major accumulation season coincides with the summer
238 precipitation due to the south-west monsoon.



239 **Fig. 8: Percentage catchment area under cloud cover has been analysed for the year**
240 **2014 over four study areas a) Durung Drung (DD) glacier, b) Chhota Shigri (CS) glacier,**
241 **c) Gangotri (GG) glacier and d) Zemu (ZM) glacier. The arrows are highlighting the**
242 **concentration of cloud cover and subsequent falls in snowline altitudes.**
243

244
245
246
247
248
249
250
251
252
253
254
255
256
257
258
259

The DD glacier has very short melting period and the snowline altitude attains its maxima during the cloud free window at the end of the ablation season (Figure 4 and 7). The snowline altitude starts to decrease with the appearance of the cloud which usually precipitates solid mass over the glacier and brings the snowline to the lower altitude from the month of October. The similar pattern is also observed for the other glaciers. However, differences are observed in the duration of the melting periods. The melting period of the ZM glacier is more than 200 days in a year which is the highest among the study areas. Table 4 has summarized the major ablation and accumulation seasons and the numbers of day's glaciers are exposed for melting. Obvious differences have been observed in the ablation and accumulation patterns. Variation in the accumulation rate, during the major accumulation season, affects the mass balance rates within the glaciers.

Table 4 Major ablation and accumulation seasons derived from snowlines and cloud cover patterns of the four glaciers (DD = Durung Drung; CS = Chhota Shigri; GG = Gangotri; ZM = Zemu).

Name of Glaciers	Major ablation season	Major accumulation season	Melting period in days
DD	Middle of June - End of August	Starting of September - Middle of June	75
CS	Middle of May - End of August	Middle of September - Middle of May	100
GG	Starting of May - End of August	Middle of September - End of April	120
ZM	Starting of April - End of September	Starting of October - End of March*	200

260
261
262
263
264
265
266
267
268
269
270
271
272
273
274
275
276
277
278
279
280
281
282
283
284
285
286
287
288
289

*Very low rate of winter accumulation comparing with other three glaciers; precipitation takes place during summer also.

5. CONCLUSIONS

The use of SAR data for estimating mass balances of glaciers facilitates regular monitoring. Monitoring of mass balance data for the high altitude Himalayan glaciers at yearly basis can provide a complete glacier inventory which is still limited by the using either optical remote sensing data or field in-situ data. The years 2014 and 2015 have better mass balance for all of the four glaciers than the previous two years. The mean of mass balances of the glaciers during the study period is $-0.44 \text{ m w.e.a}^{-1}$. The individual mass balance figure varies significantly from west to east part of the Himalaya. Average yearly mass balance of the Durung Drung and Chhota Shigri glaciers, situated at western part of the Himalaya are -0.22 and $-0.38 \text{ m w.e.a}^{-1}$, whereas, the Gangotri and Zemu glaciers are losing mass at an average rate of 0.56 and $0.60 \text{ m w.e.a}^{-1}$. This study also shows variations in the cloud cover over the study areas. The Durung Drung glacier of the western Himalaya has highest occurrence of cloud throughout the year which also helps to accumulate more solid precipitation over the glacier and improves mass balance. In contrast to the western glaciers, the cloud cover over the Zemu glacier is concentrated, especially, during the summer season. The Zemu glacier has very low amount of cloud cover during the winter time which accumulates small amount of solid mass. Lower rate of winter mass accumulation and high rate of summer precipitation may be the cause of more negative mass balance in the eastern Himalayan glaciers. However, the effects of cloud cover and precipitation over the glaciers require a detailed study over the high altitude Himalayan region. Use of the SAR data to estimate mass balance of the Himalayan glaciers increases scope to generate large amount of data in glacier inventory yearly. Regular yearly monitoring of the Himalayan glaciers can provide a better understanding on the effect of sub-tropical humid climate over the high altitude mountain glaciers and their dynamics which differ from glaciers of the polar region.

290
291
292
293
294
295
296
297
298
299
300
301
302
303
304
305
306
307
308
309
310
311
312
313
314
315
316
317
318
319
320
321
322
323
324
325
326
327
328
329
330
331
332
333
334
335
336
337
338
339
340
341
342
343
344
345
346
347

REFERENCES

1. Dobhal, D.P., Gergan J.T. and Thayyen, R.J. Mass balance studies of the Dokriani Glacier from 1992 to 2000, Garhwal Himalaya, India Bulletin of Glaciological Research. 2008:25, 9 -17.
2. Azam, M. F., Wagnon, P., Ramnathan, A., Vincent, C., Sharma, P., Arnaud, Y., Linda, A., Pottakkal, J. G., Chevallier, P., Singh, V. B. and Berthier, E. From balance to imbalance: a shift in the dynamic behaviour of Chhota Shigri glacier, western Himalaya, India. Journal of Glaciology. 2012:58 (208) [doi: 10.3189/2012JoG11J123].
3. Solomon, S. and 7 others eds. Climate change 2007: the physical science basis. Contribution of Working Group I to the Fourth Assessment Report of the Intergovernmental Panel on Climate Change. Cambridge University Press, Cambridge. 2007.
4. Cogley JG, Kargel JS, Kaser G and Van der Veen CJ. Tracking the source of glacier misinformation. Science. 2010:327(5965), 522.
5. Savoskul, O. S. and Smakhtin, V. Glacier systems and seasonal snow cover in six major Asian river basins: water storage properties under changing climate. Colombo, Sri Lanka: International Water Management Institute (IWMI)., IWMI Research Report 2013:149, 69p. [doi:10.5337/2013.203].
6. Das, S. and Chakraborty, M. Mass balance of Chhota Shigri glacier using dual-polarized C band SAR data, Remote Sensing Applications: Society and Environment. 2019:13, 150–157.
7. Berthier, E.; Arnaud, Y.; Kumar, R.; Ahmad, S.; Wagnon, P.; Chevallier, P. Remote sensing estimates of glacier mass balances in the Himachal Pradesh (Western Himalaya, India), Remote Sensing of Environment. 2007:108, 327-338.
8. Kaab, A., Berthier, E., Nuth, C., Gardelle, J. and Arnaud, Y. Contrasting patterns of early twenty-first-century glacier mass change in the Himalayas, Nature. 2012:488, 495 – 498.
9. Bolch, T., Kulkarni, A., Kääb, A., Huggel, C., Paul, F., Cogley, J. G., Frey, H., Kargel, J. S., Fujita, K., Scheel, M., Bajracharya, S. and Stoffel, M. The state and fate of Himalayan Glaciers, Science. 2012:336, 310 -314.
10. Hewitt, K. The Karakoram Anomaly? Glacier Expansion and the 'Elevation Effect,' Karakoram Himalaya. Geography and Environmental Studies Faculty Publications, Paper 8. 2005.
11. Hewitt, K. Tributary glacier surges: An exceptional concentration at Panmah Glacier, Karakoram Himalaya, Journal of Glaciology. 2007: 53 (181), 181–188.
12. Vohra, C.P. Himalayan glaciers. In: Iyer .R. ed. Harnessing the eastern Himalayan rivers, Konark Publishers Pvt. Ltd., New Delhi. 1996:120-142.
13. Ageta, Y. and Pokhral, A. P. Characteristics of mass balance components of summer-accumulation-type glacier in the Nepal Himalaya, Seppyo. 1999:45, 81-105.
14. Kundu, S. & Chakraborty, M. Delineation of glacial zones of Gangotri and other glaciers of Central Himalaya using RISAT-1 C-band dual-pol SAR, International Journal of Remote Sensing. 2015:36(6), 1529-1550.

- 348
349
350
351
352
353
354
15. Kulkarni, A. V., Rathore, B. P. and Alex, S. Monitoring of glacial mass balance in the Baspa basin using accumulation area ratio method, *Current Science*. 2004:86(1), 185 - 190.
 16. Bahuguna, I. M., Rathore, B. P., Bhambhatt, R., Sharma, M., Dhar, S., Randhawa, S. S., Kumar, K., Romshoo, S., Shah, R. D. and Ganjoo, R. K. Are the Himalayan glaciers retreating? *Current Science*. 2014:106(7), 1008-1013.

UNDER PEER REVIEW